Investigation of molybdenum and caesium behaviour in urania by *ab initio* calculations

2009 J. Phys.: Condens. Matter 21 285602

(http://iopscience.iop.org/0953-8984/21/28/285602)

J. Phys.: Condens. Matter **21** (2009) 285602 (9pp) doi:10.1088/0953-8984/21/28/285602

Investigation of molybdenum and caesium behaviour in urania by *ab initio* calculations

G Brillant[1], F Gupta[1] and A Pasturel[2,3]

[1] Institut de Radioprotection et de Sûreté Nucléaire, DPAM, SEMIC, LETR, BP 3, F-13115 Saint-Paul-Lez-Durance Cedex, France
[2] Sciences et Ingénierie des Matériaux et Procédés, INP Grenoble, UJF-CNRS, 1130 rue de la Piscine, BP 75, F-38402 Saint-Martin d'Hères Cedex, France
[3] Laboratoire de Physique et Modélisation des Milieux Condensés, Maison des Magistères, BP 166 CNRS, F-38042 Grenoble Cedex 09, France

E-mail: guillaume.brillant@irsn.fr

Received 26 February 2009, in final form 21 April 2009
Published 18 June 2009
Online at stacks.iop.org/JPhysCM/21/285602

Abstract
A theoretical study of molybdenum and caesium solution in uranium dioxide is carried out. Calculations are performed using the density functional theory with the projector-augmented-wave method as implemented in the Vienna *ab initio* simulation package (VASP). Correlation effects are taken into account within the DFT + U approach. Molybdenum is preferentially inserted in uranium–oxygen divacancies for understoichiometric urania and uranium vacancies for overstoichiometric urania. The favourable sites for caesium solution are the Schottky defect for understoichiometric urania and U vacancies and U–O divacancies for overstoichiometric urania. Using the stability of many binary and ternary compounds in comparison to soluted atoms, we show that caesium and molybdenum are insoluble in uranium dioxide whatever the stoichiometric regime.

(Some figures in this article are in colour only in the electronic version)

1. Introduction

Understanding the fission products' (FP) behaviour is crucial for the source term evaluation in the case of a hypothetical severe accident at a nuclear power plant. Nuclear power plant safety studies more and more require advanced interpretations of the complex phenomena involved in FP release from fuel. For setting up models of FP release kinetics, FP location within fuel and stable FP chemical forms have to be determined. In that view, *ab initio* calculations can be performed to find out whether a fission product is likely to be soluted in the fuel lattice or in precipitates. However, theoretical studies of UO_2 are known to be difficult. Interionic empirical potentials using Mott–Littleton methodology were first used to estimate defect formation energies or some FP solution energies [1–6]. Because of the inherent approximations made in such calculations, some significant discrepancies with experimental surveys can be noticed. More recently, *ab initio* calculations, based on density functional theory, were used to model the behaviour of Kr [7], He and Xe [8] and Kr, I, Cs, Sr and He [9] in UO_2. However, these calculations used both the local density approximation (LDA) and generalized gradient approximation (GGA) which are known to give a qualitatively incorrect description of the strongly correlated 5f electrons of uranium. In fact, the 5f electrons can either be localized or contribute to bonding and electronic–electronic correlations are very important factors in deciding the degree of localization. In order to better take into account the localization of uranium f-electrons, the GGA + U functional can be considered. Indeed, we showed that the use of the GGA + U functional leads to a better agreement with experimental measurements for the energies of defect formations [10] and of fission products' solutions in uranium dioxide [11, 12]. In this contribution, calculations with the GGA + U exchange–correlation functional have been performed to evaluate the solution energies in UO_2 of the two important fission products, which are Mo and Cs.

Beyond its high fission yield and radiological effects, molybdenum is an important fission product as far as fuel oxidation is considered. As a matter of fact, the Mo/MoO_2

couple is known to have a buffering effect on the fuel oxygen potential evolution [13–15]. Moreover, molybdenum may play a role in some FP release by chemical interactions and compounds formation (with caesium, strontium or barium, for instance). In fuel, molybdenum has a low solubility [16, 17, 3] and is mainly observed in metallic or oxide precipitates [18–20]. In accidental conditions, caesium is released rapidly and in large quantities, and has, mainly due to its isotope ^{137}Cs, a high radiological impact on human health and the environment. Caesium has a low solubility in nuclear fuel [21, 17, 22]. It is mainly observed dissolved in the matrix or in gas bubbles and has similarities with the rare gases. Nevertheless, caesium is suspected to participate in the formation of precipitates of caesium uranates and molybdates [23, 18, 24, 19, 25, 26].

Firstly, the numerical methodology employed in the present work is described. Then, incorporation and solution energies of Mo and Cs in pre-existing trap sites of UO_2 are evaluated and impact of temperature and fuel deviation from stoichiometry is discussed. Lastly, the solubility of caesium and molybdenum in urania is studied using the determination of the stability of many binary and ternary compounds in comparison with soluted atoms.

2. Methodology

Calculations of total energies are carried out using density functional theory (DFT) with the projector-augmented-wave method [27] as implemented in the Vienna *ab initio* simulation package (VASP) [28]. All the calculations are performed within DFT with the generalized gradient GGA + U approximation that takes into account the electronic correlation present in UO_2. The Hubbard U correction is introduced to describe strongly correlated uranium 5f electrons. Hence the localized electrons (5f) experience a spin- and orbital-dependent potential, while the other orbitals are delocalized and considered to be properly described by GGA. The rotationally invariant form of GGA + U is used with a spherically averaged double-counting term [29]. Within this approximation, there is a single parameter U_{eff} which is chosen to be equal to 4 eV for all the studied compounds. Such a value is also very close to the value used by Dudarev *et al* [30] or by Laskowski *et al* [31] and to the experimental findings [32, 33]. It has been shown that such an approximation provides a correct description of electronic, magnetic and cohesive properties of UO_2 [10].

A plane wave basis set with a cutoff energy of 480 eV was used in all calculations. Numerical integrations in the Brillouin zone (BZ) were performed by means of the Hermite–Gaussian method with $N = 1$ and a smearing parameter of $\sigma = 0.001$ eV. BZ sampling using a $4 \times 4 \times 4$ k-point grid was found necessary for differences of total energies and magnetic moments of our $2 \times 2 \times 2$ cubic cell of UO_2 (96 atoms) to converge within 10^{-3} eV and 0.01 μ_B, respectively. Structural optimizations were carried out at constant volume and under the condition that all residual forces should be smaller than 0.01 eV Å^{-1}. The constraint of constant volume is well adapted to describing the solution of fission products in urania in the limit of dilute defect concentrations. Indeed, in such conditions, no drastic modification of the long range lattice parameter is expected [34]. In our previous study [12], we checked that adding one barium atom in the supercell of 96 atoms leads only to very small variations in the equilibrium volume. Let us mention that, at high concentrations, fuel swelling can be expected. In this case, the volume constant constraint is no longer valid and a constant pressure constraint would be preferable, as proposed by Iwasawa *et al* [35]. However, such a study is not the objective of this work. The volume is fixed, using the equilibrium lattice constant, to 5.52 Å and the antiferromagnetic (AF) structure found at very low temperature was assumed [10]. At $T = 30.8$ K, UO_2 undergoes a discontinuous transition from the antiferromagnetic state to a paramagnetic state for which modelling is beyond the scope of our calculations. However, the energy differences between different magnetic configurations have been found to be small [10, 36]. These results indicate that the long range magnetic ordering has only minor effects on the cohesive properties of UO_2. Therefore, calculations of defect energies using the AF configuration can be considered as being still valid at high temperatures. Finally, even if entropy calculations should be considered to fully study the fission products' solution in uranium dioxide, we have neglected them hereafter.

3. Mo and Cs incorporation in the UO_2 lattice

3.1. Incorporation energies

The incorporation energies of molybdenum and caesium in the UO_2 lattice are evaluated using the 96-atom supercell. Incorporation sites consist of the interstitial position (Int) and the following crystallographic defects: the oxygen and uranium vacancies (V_O and V_U), the oxygen–uranium divacancy (DV) and the Schottky defect (Sch) or neutral trivacancy. Three different configurations exist for the Schottky defect [12]. However, since the incorporation energies of other FPs have been found to be similar for all these configurations [12] only the configuration characterized by the angle of 70° between the two V_O–V_U axes has been used in the present calculations. The incorporation energy of molybdenum is estimated using the following formula:

$$E^{\text{inc}}_{\text{Mo}\in\text{X}} = E_{\text{Mo}\in\text{X}} - E_{\text{X}} - E^{\infty}_{\text{Mo}} \quad (1)$$

where $E_{\text{Mo}\in\text{X}}$ is the energy of the supercell containing Mo in site X; E_{X} is the energy of the supercell containing a defect site of type X and E^{∞}_{Mo} is the energy of the isolated Mo atom. Note that the stability of molybdenum and caesium in fuel, including the formation of binary or ternary compounds, is discussed in the next paragraph.

The incorporation energies after relaxation as well as relaxation energies for molybdenum and caesium are reported in table 1. Since the constant volume constraint is imposed, the relaxation energies are related to the ionic contribution at a fixed lattice parameter. First we note that relaxation energies are important, such effects being greater for caesium than for molybdenum. Moreover, these effects are particularly high for

Table 1. Incorporation and relaxation energies (eV) of Mo and Cs in the UO_2 lattice.

	Mo		Cs	
X	E_X^{inc}	E_X^{relax}	E_X^{inc}	E_X^{relax}
Int	−0.9	−3.5	7.5	−4.8
V_O	1.7	−2.9	6.4	−9.3
V_U	−7.6	−3.7	−1.2	−4.7
DV	−6.4	−2.4	−1.1	−4.6
Sch	−3.1	−4.6	−0.6	−4.4

the incorporation energy of caesium in the oxygen vacancy site as found also for Ba [12]. For both caesium and molybdenum atoms, our findings are that the lowest incorporation energy corresponds to the uranium vacancy, followed by the divacancy and Schottky defects. The incorporation energies as well as related relaxation energies can be understood on the basis of a competition between size effects due to the incorporation of the FP products and bond formation of these FP products with neighbouring oxygen atoms. The incorporation energies of molybdenum are negative for all defective sites except for the oxygen vacancy site. These results indicate an easy incorporation of molybdenum in UO_2, which is consistent with the possibility of molybdenum to have an oxidation number of +IV like uranium. The larger size of caesium atoms relative to uranium atoms leads to size effects that increase the competition between chemical and steric effects similar to that due to the barium incorporation [12]. For barium, chemical interactions were found to remain the main factor to interpret its incorporation in UO_2. For caesium, these chemical interactions are smaller since the incorporation energies of caesium are much less negative. Such more positive incorporation energies of caesium can be related to the fact that Coulombic effects between barium and oxygen atoms are more important than those found between Cs and O atoms as noted by Grimes *et al* [4]. Finally, we note that our calculated values of incorporation energies of caesium are in qualitative agreement with those obtained by using Mott–Littleton methodology. Within this approach, the incorporation energy of caesium is calculated to be positive in Int and V_O and negative in V_U, DV and Sch. We find more discrepancies with other DFT-based calculations such as those reported in [9]. However, we have to emphasize that relaxation effects were not taken into account in these calculations which explains the high positive values obtained for all the defective sites.

3.2. Solution energies

Comparison of incorporation energies is the simplest way to determine FP stabilities in UO_2. However, their use is limited since they are not sensitive to concentrations of the different insertion sites. To take into account this concentration dependence, it is necessary to evaluate the solution energy. This energy can be defined as follows:

$$E^{sol}_{Mo\in X} = E^{inc}_{Mo\in X} + E^{Fapp}_X \tag{2}$$

where E_X^{Fapp} is the apparent formation energy of defect X. Note that E_X^{Fapp} depends on temperature and on the deviation from stoichiometry through the following expression:

$$E_X^{Fapp} = -kT\ \log([X]). \tag{3}$$

Apparent formation energies can be evaluated in the framework of the point defect model (PDM) introduced by Matzke [37] and Lidiard [38] to obtain the concentration of defects in UO_2 and their dependence with stoichiometry. This model is based on the assumption that the defects responsible for the deviation from stoichiometry in UO_2 are isolated point defects. Even if it had been known for a long time that oxygen interstitials form clusters of defects, this model is commonly used to analyse the variation of the populations of point defects with stoichiometry or oxygen pressure. Very recently, Geng *et al* [39] showed that PDM can be used for $x < 0.03$, in agreement with the experimental fact. Within PDM, the concentration of defects in urania is estimated using the following approximation: major defects are the oxygen vacancies in UO_{2-x}, the oxygen Frenkel pairs in UO_2 and the oxygen interstitials in UO_{2+x}. Using this basic model, one can easily estimate E^{Fapp} (see table 2). Solution energies from our calculations are reported in table 3.

Molybdenum is found to be preferentially inserted in a divacancy for understoichiometric and stoichiometric urania and in a uranium vacancy for overstoichiometric uranium dioxide. This is in qualitative agreement with calculations carried out with Mott–Littleton methodology [3] (favourable sites are Sch in UO_{2-x}, DV and Sch in UO_2 and V_U in UO_{2+x}). Even if molybdenum appears to be much less soluble with the Mott–Littleton approach than with the DFT-GGA + U method, our results support experimental features that show the solubility of Mo by XANES (x-ray absorption near-edge structure) after ion implantation in stoichiometric uranium dioxide [20].

Favoured solution sites for caesium are Sch for UO_{2-x}, Sch and DV for UO_2 and DV and V_U for UO_{2+x}. Solution energies of caesium are higher than molybdenum ones and are only negative for V_U and DV in overstoichiometric fuel. This is in qualitative agreement with interionic pseudopotential calculations [4, 40]. However, their calculated energy for caesium solution in V_U ($E^{sol}_{V_U} = -6.4$ eV) is much more negative than ours. Theoretical results are also in good agreement with experimental features since it has been observed experimentally that Cs has a low solubility in nuclear fuels (0.07 mass% Cs in UO_2 at 2173 K [17]).

To go beyond approximations made in the point defect model, one has to solve the equation system (4) where $[I_{O,U}]$ and $[V_{O,U}]$ are interstitial and vacancy concentrations of oxygen and uranium, [DV] is the divacancy concentration and [Sch] is the Schottky concentration:

$$[V_O][I_O] = \exp\left(-\frac{E_{PF_O}}{k_B T}\right) \tag{4a}$$

$$[V_U][I_U] = \exp\left(-\frac{E_{PF_U}}{k_B T}\right) \tag{4b}$$

$$[V_O]^2[V_U] = \exp\left(-\frac{E_{Sch}}{k_B T}\right) \tag{4c}$$

Table 2. Apparent formation energies of defects in uranium dioxide.

	$E_X^{F\,app}$		
X	UO_{2-x}	UO_2	UO_{2+x}
V_O	$-kT\ln(\lvert x\rvert/2)$	$\frac{E_{PF_O}}{2}+\frac{kT}{2}\ln(2)$	$E_{PF_O}+kT\ln(x)$
V_U	$2kT\ln(\frac{\lvert x\rvert}{2})+E_{Sch}$	$E_{Sch}-E_{PF_O}-kT\ln(2)$	$E_{Sch}-2E_{PF_O}-2kT\ln(x)$
DV	$E_{Sch}-B_{DV}+kT\ln(\frac{\lvert x\rvert}{2})$	$E_{Sch}-\frac{E_{PF_O}}{2}-B_{DV}-\frac{kT}{2}\ln(2)$	$E_{Sch}-E_{PF_O}-B_{DV}-kT\ln(x)$
Sch	$E_{Sch}-B_{Sch}$	$E_{Sch}-B_{Sch}$	$E_{Sch}-B_{Sch}$

Table 3. Solution energies (eV) of Mo and Cs in $UO_{2\pm x}$ at $T = 0$ K using the formula given in table 2 (bold values indicate the most favourable site).

E_X^{sol}	Mo			Cs		
X	UO_{2-x}	UO_2	UO_{2+x}	UO_{2-x}	UO_2	UO_{2+x}
Int	−0.9	−0.9	−0.9	7.5	7.5	7.5
V_O	1.7	3.7	5.7	6.4	8.4	10.4
V_U	−0.4	−4.4	**−8.4**	6.1	2.0	**−2.0**
DV	**−3.1**	**−5.1**	−7.1	2.2	**0.2**	−1.8
Sch	−1.6	−1.6	−1.6	**0.9**	0.9	0.9

$$[DV] = [V_O][V_U]\exp\left(-\frac{B_{DV}}{k_B T}\right) \tag{4d}$$

$$[Sch] = [V_O]^2[V_U]\exp\left(-\frac{B_{Sch}}{k_B T}\right) \tag{4e}$$

$$2[V_U] + [I_O] \simeq 2[I_U] + 2[V_O] + x \tag{4f}$$

where E_{PF_O} and E_{PF_U} are the energies of the oxygen and uranium Frenkel pairs' formation, E_{Sch} is the Schottky defect formation energy, and B_{DV} and B_{Sch} are the binding energies of di- and trivacancies. To solve this set of equations, one can make the less restrictive assumption, which is to neglect the uranium interstitial concentration in comparison to other defect concentrations. This assumption, which is verified *a posteriori*, leads to the following cubic equation:

$$P(Y = [V_O]) = 0 = 2Y^3 + xY^2 - Y\exp\left(-\frac{E_{PF_O}}{k_B T}\right) - 2\exp\left(-\frac{E_{Sch}}{k_B T}\right). \tag{5}$$

Since the polynomial equation verifies the following conditions (where Y_1 and Y_2 are the two roots of $\frac{dP}{dY} = 0$):

$$Y_1 < 0 \qquad \text{and} \qquad Y_2 > 0 \tag{6a}$$

$$P(0) < 0 \tag{6b}$$

it has a unique positive solution $Y_0 = [V_O]$ which can be written as

$$[V_O] = (q+p)^{1/3} + (q-p)^{1/3} - \frac{x}{6} \tag{7}$$

with q and p defined as

$$q = \frac{\exp(-E_{Sch}/kT)}{2} - \frac{x\,\exp(-E_{FP_O}/kT)}{12} - \frac{x^3}{216} \tag{8a}$$

$$p = \left[q^2 - \left(\frac{6\,\exp(-E_{FP_O}/kT) + x^2}{36}\right)^3\right]^{1/2}. \tag{8b}$$

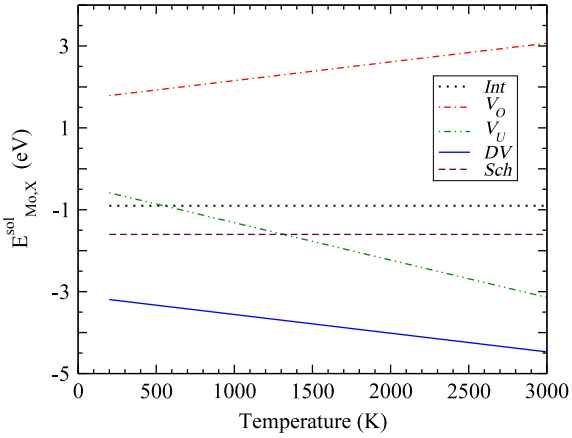

Figure 1. Temperature impact on the solution energies of molybdenum in $UO_{1.99}$.

The other defect concentrations can be determined either using equations from system (4) or directly using a similar method as for $[V_O]$. Note that, for overstoichiometric fuel, oxygen vacancies are not the dominant defect and some numerical errors can appear. To avoid these errors, the oxygen interstitial concentration has to be calculated first.

The evolution of the solution energies of molybdenum with temperature for $UO_{1.99}$ is plotted in figure 1. The main result is that the divacancy defect is stable over the whole range of studied temperatures and the solution energy of Mo in this site becomes more and more negative. The apparent formation energy of the Schottky defect is constant whatever the temperature and the stoichiometric deviation. In contrast, at a fixed stoichiometric deviation for understoichiometric uranium dioxide, the apparent formation energy of uranium vacancies goes down as temperature goes up. As a consequence, the solution energy of molybdenum in a uranium vacancy displays a very strong temperature dependence and becomes lower than the solution energy in the Schottky defect at temperatures greater than 1300 K. We can even suspect that the role of the uranium vacancy becomes important at very high temperatures, corresponding to the conditions of a severe nuclear accident. The situation is quite different for the solubility of Cs in $UO_{1.99}$ (see figure 2) since the solution energies for all the insertion sites are positive in the whole range of temperatures. We can note that the divacancy is preferred to the Schottky defect for temperatures greater than 2800 K.

The variation of the solution energies of molybdenum with stoichiometry at $T = 2000$ K are drawn in figure 3. One can observe an important stability range of the divacancy

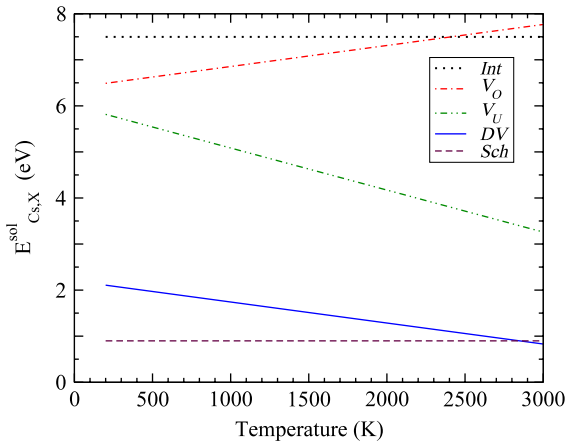

Figure 2. Temperature impact on the solution energies of caesium in $UO_{1.99}$.

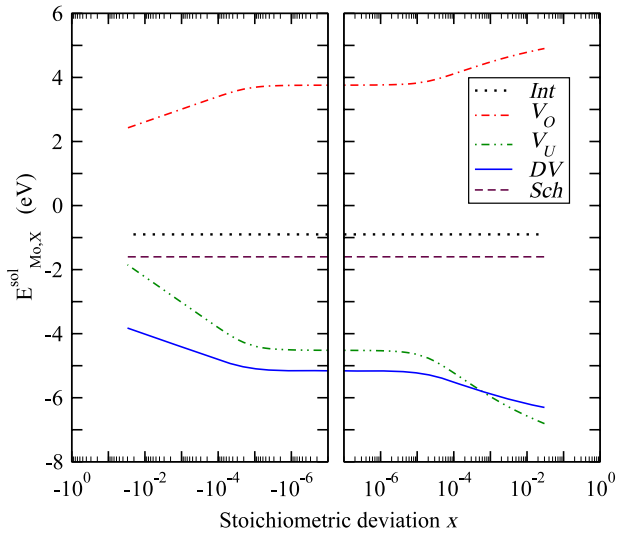

Figure 3. Impact of the fuel stoichiometric deviation on the solution energies of molybdenum in uranium dioxide at $T = 2000$ K.

since the uranium vacancy becomes the most favourable site only for $x > 10^{-3}$. This finding is not different from that obtained at $T = 0$ K using the PDM model. Figure 4 displays solution energies of caesium. The stability range of the divacancy is also found to be important. For this element, the competition occurs with the Schottky defect at $x = -10^{-3}$. In the overstoichiometric regime, the solution energy of the divacancy defect decreases as x increases and becomes negative for $x > 10^{-4}$. It is consistent with experimental observations of larger amounts of soluted caesium for fuels with high O/M ratios [41]. The solution energy of Cs in the divacancy is slightly higher than that in the uranium vacancy for UO_{2+x} at $T = 0$ K (see table 3). However, as temperature increases, the apparent formation energy of the uranium vacancy increases twice as fast as the apparent formation energy of the divacancy. Therefore, the divacancy rapidly becomes the most stable site for caesium solution in UO_{2+x} as temperature increases.

To conclude this part, as far as isolated atoms are considered (and not secondary phases), molybdenum is

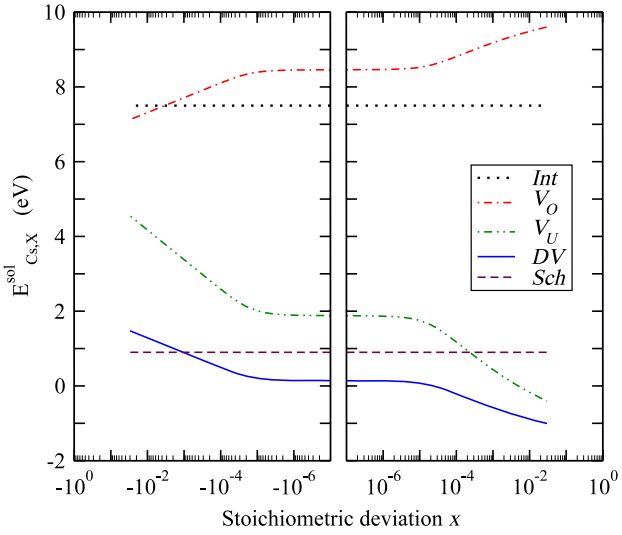

Figure 4. Impact of the fuel stoichiometric deviation on the solution energies of caesium in uranium dioxide at $T = 2000$ K.

expected to be much more soluble in uranium dioxide than caesium. In comparison with the results of [12], the solution energies of molybdenum are similar to those of barium but higher than those of zirconium.

4. Mo and Cs stability in $UO_{2\pm x}$

Previous calculations are very useful in predicting the solution site occupancy of Mo and Cs in UO_2. However, as mentioned in section 1, it is also possible that Mo and Cs precipitate out of solution in a more stable secondary phase. Although the number of possible second-phase materials that Mo and Cs can form both with each other and with other elements present in UO_2 can be very important, experimental data [23, 21, 24] suggest that the majority of these are either metallic inclusions or oxide phases.

In the following, we evaluate the stability of molybdenum and caesium in metallic precipitates, in binary oxides and in ternary compounds. Then, the solubility of Mo and Cs in uranium dioxide is discussed.

4.1. Metallic precipitates

On the basis of thermodynamic estimates of the oxygen potential of the fuel and the thermodynamics in the Cs–Mo–O–U system [42] metallic forms of both caesium and molybdenum have a domain of stability for temperatures lower than 1200 K (that is, the average temperature of the irradiated fuel) and oxygen potentials lower than -400 kJ mol^{-1}. In the following, the stability of metallic precipitates is studied in comparison with atoms soluted in their most favourable insertion sites Cs_X/Mo_X which depend on the deviation from stoichiometry. Therefore, taking the example of molybdenum, the following chemical reaction is considered:

$$Mo_{(m)} \rightarrow Mo_X$$

Table 4. Solution energies of caesium and molybdenum precipitates in $UO_{2\pm x}$.

Precipitate	E^{sol} (eV)		
	UO_{2-x}	UO_2	UO_{2+x}
$Mo_{(m)}$	3.1	1.1	−2.2
$Cs_{(m)}$	1.6	0.9	−1.3
Cs_2O	1.3	1.9	−0.5
Cs_2O_2	−2.6	0.0	−0.4
CsO_2	−5.9	−2.6	−2.8
MoO_2	−1.1	0.9	0.6
MoO_3	−4.4	−0.4	2.3
Cs_2UO_4	0.4	3.0	2.6
Cs_2ZrO_3	−3.8	2.4	0.0
Cs_2MoO_4	1.3	5.9	6.2
$BaMoO_3$	−0.5	0.7	−0.6
$BaMoO_4$	−2.2	1.0	1.7

and solution energy can be estimated through

$$E^{sol}_{Mo_{(m)}} = E^{sol}_{Mo\in X} - E^{cohe}_{Mo_{(m)}} \quad (9)$$

where E^{cohe}_{Mo} is the cohesive energy of metallic molybdenum with respect to isolated Mo and $E^{sol}_{Cs\in X}$ the solution energy of caesium in uranium dioxide in the most stable site X (X = divacancy in UO_{2-x}, for instance) as calculated in section 3. The DFT calculation of metallic molybdenum leads to a cohesive energy of −6.20 eV (exp. −6.82 eV [43]) and a lattice parameter of 3.16 Å (exp. 3.14 Å [44, 24]). Concerning metallic caesium, we calculated a cohesive energy of −0.70 eV and a lattice parameter of 6.12 Å (exp. −0.84 eV and 6.18 Å [45, 24]). Note that $E^{sol}_{Mo\in X}$ and $E^{cohe}_{Mo_{(m)}}$, $E^{sol}_{Cs\in X}$ and $E^{cohe}_{Cs_{(m)}}$ are all calculated with respect to the isolated atom. Solution energies of Cs and Mo are gathered in table 4. A positive solution energy indicates that the metallic precipitate is insoluble in the fuel. Then we can conclude that both metallic precipitates of caesium and molybdenum are found to be insoluble in UO_{2-x} and UO_2 and soluble in UO_{2+x}. This is consistent with experimental observation of inclusion in understoichiometric and near-stoichiometric fuel of an ϵ-Ru metallic phase (Ru, Pd, Rh, Tc, Mo) [18–20]. However, in the overstoichiometric regime, it is expected that the formation of metallic compounds competes with that of oxide forms and the solubility of these oxide forms also has to be analysed.

4.2. Binary oxides

Considering temperature and oxygen potential ranges encountered during normal and accidental conditions for nuclear fuel, the two more likely forms of binary oxides of caesium and molybdenum are Cs_2O and MoO_2. For very high oxygen potentials, one has to take into account MoO_3 and perhaps even Cs_2O_2 and CsO_2. Let us also mention that Mo plays a peculiar role for the fuel stoichiometry since Mo acts as a buffer in UO_2 oxidation [13–15].

The stability of precipitates of caesium oxides is studied in comparison with caesium and oxygen soluted in their most favourable insertion sites Cs_X and O_Y which depend on the stoichiometry deviation of the fuel. Therefore, taking the example of Cs_2O, the following chemical reaction is considered:

$$Cs_2O \rightarrow 2\,Cs_X + O_Y$$

and Cs_2O solution energy can be estimated through

$$E^{sol}_{Cs_2O} = 2E^{sol}_{Cs\in X} + E^{sol}_{O\in Y} - E^{cohe}_{Cs_2O} \quad (10)$$

where $E^{cohe}_{Cs_2O}$ is the cohesive energy of caesium oxide and $E^{sol}_{Cs\in X}$ is the solution energy of caesium in uranium dioxide in the most stable site X. The oxygen solution site Y depends on the stoichiometry of the fuel. In fact, considering the results of our previous study [10], oxygen is soluted into an oxygen vacancy in UO_{2-x} and UO_2, and into an oxygen vacancy and interstitial site in UO_{2+x} with the respective solution energies $E^{sol}_{O\in Y}$: −5.6, −3.6 and −1.6 eV. Note that the energies $E^{sol}_{Cs\in X}$, $E^{sol}_{O\in Y}$ and $E^{cohe}_{Cs_2O}$ are calculated with respect to isolated Cs, Mo and to O in a dioxygen molecule.

The formation energies of the different binary compounds are evaluated with VASP using the DFT-GGA approximation. For each structure, the k-point grid was chosen to give a convergence within 10^{-5} eV/atom for the total energy. Structural optimizations were carried out until all residual forces were less than 0.01 eV A^{-1}. Calculated lattice parameters and formation energies, with respect to the atomic reference state, are shown in table 5 and are compared with experimental data. Calculated structural parameters fit experiments very well while calculated formation energies are slightly more negative than experimental data.

The solution energies of all binary oxides are collected in table 4. It must be emphasized that solution energies in UO_{2-x} are not discussed since binary oxides are thermodynamically unstable for oxygen potential corresponding to understoichiometric urania. Regarding molybdenum, our findings are that MoO_2 is insoluble in UO_2 and UO_{2+x} and MoO_3 in UO_{2+x}. This is consistent with experimental evidence of precipitates of molybdenum oxides in nuclear fuels. Considering caesium, Cs_2O is found to be insoluble at stoichiometry whereas all binary oxides are soluble in overstoichiometric fuel. However, the formation of some ternary compounds can prevent the solution of caesium in urania.

4.3. Ternary compounds

In this section, we study the influence of the most important ternary compounds on the solubility of Mo and Cs in fuel. More particularly, we focus our attention on the behaviour of ternary compounds occurring between Mo and Cs but also including Ba and Zr, elements studied in our previous contribution [12]. These compounds are Cs_2UO_4, Cs_2ZrO_3, Cs_2MoO_4, $BaMoO_3$ and $BaMoO_4$ and their solubility is evaluated using similar chemical reactions as described for binary oxides. Therefore, taking the example of Cs_2MoO_4, the following chemical reaction is considered:

$$Cs_2MoO_4 \rightarrow 2\,Cs_X + Mo_Z + 4O_Y$$

and Cs_2MoO_4 solution energy can be estimated through

$$E^{sol}_{Cs_2MoO_4} = 2E^{sol}_{Cs\in X} + E^{sol}_{Mo\in Z} + 4E^{sol}_{O\in Y} - E^{cohe}_{Cs_2MoO_4} \quad (11)$$

Table 5. Binary and ternary compound characteristics.

		Lattice parameters (Å)		Formation energies (eV)	
	Group	Calc.	Exp.	Calc.	Exp.
Cs_2O	$R\bar{3}m$	$a = 4.26$ $c = 19.01$	$a = 4.256$ $c = 18.99$	−3.65	−3.59 [24]
Cs_2O_2	$Immm$	$a = 4.27$ $b = 7.47$ $c = 6.480$	$a = 4.322$ $b = 7.517$ $c = 6.430$	−5.35	−5.01 [23]
CsO_2	$I4/mmm$	$a = 4.39$ $b = 7.30$	$a = 4.477$ $b = 7.350$	−3.64	−3.06 [46]
MoO_2	$P2_1/c$	$a = 5.61$ $b = 4.89$ $c = 5.66$ $\beta = 121°$	$a = 5.611$ $b = 4.856$ $c = 5.629$ $\beta = 120.95°$	−6.97	−6.11 [24]
MoO_3	$Pnma$	$a = 13.90$ $b = 3.71$ $c = 3.92$	$a = 13.86$ $b = 3.696$ $c = 3.963$	−9.27	−7.72 [24]
Cs_2UO_4	$I4/mmm$	$a = 4.43$ $c = 14.61$	$a = 4.392$ $c = 14.80$	−19.51	−19.98 [24]
Cs_2MoO_4	$Pnma$	$a = 8.46$ $b = 6.48$ $c = 11.46$	$a = 8.510$ $b = 6.562$ $c = 11.61$	−17.28	−15.70 [24]
Cs_2UO_4	$I4/mmm$	$a = 11.28$ $b = 7.68$ $c = 5.97$	$a = 11.27$ $b = 7.743$ $c = 5.956$	−16.48	−16.43 [24]
$BaMoO_3$	$Pm\bar{3}m$	$a = 4.05$	$a = 4.05$	−13.76	−12.73 [24]
$BaMoO_4$	$I4_1/a$	$a = 5.57$ $c = 12.69$	$a = 5.548$ $c = 12.74$	−17.64	−16.02 [24]

where $E^{\text{cohe}}_{Cs_2MoO_4}$ is the cohesive energy of caesium molybdate, $E^{\text{sol}}_{Cs\in X}$ the solution energy of caesium in uranium dioxide in the most stable site X (X = divacancy in UO_{2-x}, for instance), $E^{\text{sol}}_{Mo\in Z}$ the solution energy of molybdenum in uranium dioxide in the most stable site Z (Z = Schottky defect in UO_{2-x}) as calculated in section 3 and $E^{\text{sol}}_{O\in Y}$ the solution energy of oxygen in uranium dioxide in the most stable site Y (Y = oxygen vacancy in UO_{2-x}), which is calculated using previous results [10]. Calculations of $E^{\text{cohe}}_{Cs_2MoO_4}$, $E^{\text{sol}}_{Cs\in X}$, $E^{\text{sol}}_{Mo\in Z}$ and $E^{\text{sol}}_{O\in Y}$ are performed with respect to isolated Cs, Mo and to O in a dioxygen molecule. It should be noted that for Cs_2UO_4, the following reaction is considered:

$$Cs_2UO_4 \rightarrow 2Cs_X + 2O_Y + UO_2.$$

Besides, solution energies of barium and zirconium are extracted from [12]. Formation energies of ternary compounds were computed using the same approximations than for binary compounds. In table 5, we report both calculated and experimental lattice parameters and formation energies of these different compounds. Note that lattice parameters are experimentally measured at room temperature while *ab initio* calculations are performed at 0 K. Then calculated solution energies of ternary compounds are gathered in table 4. Caesium ternary compounds are found to be insoluble in $UO_{2\pm x}$ except caesium zirconate in UO_{2-x}. However, from a thermodynamic point of view, Cs_2ZrO_3 is unstable for oxygen potential corresponding to understoichiometric urania. Therefore, our results are in agreement with experimental observations of low caesium solubility in urania [17, 22] and of formation of caesium uranates in nuclear fuels [18, 47–51].

Concerning molybdenum, Cs_2MoO_4 is insoluble in $UO_{2\pm x}$ as $BaMoO_4$ in UO_2 and UO_{2+x} while the solution energy of $BaMoO_3$ is close to zero. Using our results based on solution energies of metallic and binary oxide forms of molybdenum, it can be concluded that the solubility of molybdenum is weak in nuclear fuels as experimentally observed [16, 17]. Moreover, the present study including ternary compounds with Ba and Zr completes the conclusions of [12]. Indeed the solubility of barium and zirconium in stoichiometric and overstoichiometric fuels can be reduced by the formation of Cs_2ZrO_3 and $BaMoO_4$ compounds when fission products can meet.

5. Conclusions

Ab initio calculations of the incorporation and solution energies of caesium and molybdenum in uranium dioxide have been carried out using the DFT method with the GGA + U exchange–correlation functional. We find that the most favourable solution sites of Mo is the U–O divacancy for UO_{2-x} and UO_2 and the U vacancy for UO_{2+x}. Caesium is preferentially inserted in a Schottky defect for UO_{2-x}, in a U–O divacancy for UO_2 and in a U vacancy for UO_{2+x}. We put in evidence that (i) the solubility of both Cs and Mo atoms is facilitated by increasing temperature and deviation from stoichiometry and (ii) chemical interactions are the most important effect for molybdenum whereas steric constraints become predominant for caesium.

To go beyond the evaluation of isolated atoms' solution in the urania lattice, we have studied the stability of major

secondary phases observed in nuclear fuels. We conclude that the solubility of both caesium and molybdenum is low in uranium dioxide. Caesium may precipitate in rare gas bubbles or under caesium uranates or molybdates and molybdenum under metallic phases for understoichiometric fuel and oxide phases for overstoichiometric fuel.

Finally, let us emphasize that this study shows how *ab initio*-based data may be generated from which thermodynamic models predicting solubility of fission products can be developed. A complete study including other major fission products will be carried out to elucidate the complexity of this phenomenon.

References

[1] Catlow C R A 1973 Defect clusters in doped fluorite crystals *J. Phys. C: Solid State Phys.* **6** 64–70

[2] Goff J P, Fåk B, Hayes W and Hutchings M T 1992 Defect structure and oxygen diffusion in $UO_{2+\delta}$ *J. Nucl. Mater.* **188** 210–5

[3] Nicoll S, Matzke H, Grimes R W and Catlow C R A 1997 The behaviour of single atoms of molybdenum in urania *J. Nucl. Mater.* **240** 185–95

[4] Grimes G W and Catlow C R A 1991 The stability of fission products in uranium dioxide *Phil. Trans. R. Soc.* A **335** 609–34

[5] Morelon N-D, Ghaleb D, Delaye J-M and Van Brutzel L 2003 A new empirical potential for simulating the formation of defects and their mobility in uranium dioxide *Phil. Mag.* **83** 1533–50

[6] Govers K, Lemehov S, Hou M and Verwerft M 2007 Comparison of interatomic potentials for UO_2. Part I: static calculations *J. Nucl. Mater.* **366** 161–77

[7] Petit T, Jomard G, Lemaignan C, Bigot B and Pasturel A 1999 Location of krypton atoms in uranium dioxyde *J. Nucl. Mater.* **275** 119–23

[8] Freyss M, Vergnet N and Petit T 2006 *Ab initio* modeling of the behavior of helium and xenon in actinide dioxide nuclear fuels *J. Nucl. Mater.* **352** 144–50

[9] Crocombette J P 2002 *Ab initio* energetics of some fission products (Kr, I, Cs, Sr, and He) in uranium dioxide *J. Nucl. Mater.* **305** 29–36

[10] Gupta F, Brillant G and Pasturel A 2007 Correlation effects and energetics of point defects in uranium dioxide: a first principle investigation *Phil. Mag.* **87** 2561–9

[11] Gupta F 2008 Etude du comportement du produit de fission cesium dans le dioxide d'uranium par methode *ab initio PhD Thesis* Paris XI

[12] Brillant G and Pasturel A 2008 Study of barium and zirconium stability in $UO_{2\pm x}$ by density functional calculations *Phys. Rev.* B **77** 184110

[13] Matzke H 1995 Oxygen potential measurements in high burn-up LWR UO_2 fuel *J. Nucl. Mater.* **223** 1–5

[14] Park K, Yang M-S and Park H-S 1997 The stoichiometry and the oxygen potential change of urania during irradiation *J. Nucl. Mater.* **247** 116–20

[15] Serrano J A, Glatz J P, Toscano E H, Barrera J and Papaioannou D 2001 Influence of low-temperature air oxidation on the dissolution behaviour of high burn-up LWR spent fuel *J. Nucl. Mater.* **294** 339–43

[16] Giachetti G and Sari C 1976 Behavior of molybdenum in mixed-oxide fuel *Nucl. Technol.* **31** 62–9

[17] Kleykamp H 1993 The solubility of selected fission products in UO_2 and (U, Pu)O_2 *J. Nucl. Mater.* **206** 82–6

[18] Kleykamp H 1985 The chemical state of the fission products in oxide fuels *J. Nucl. Mater.* **131** 221–46

[19] Sato I, Furuya H, Idemitsu K, Arima T, Yamamoto K and Kajitani M 1997 Distribution of molybdenum in FBR fuel irradiated to high burnup *J. Nucl. Mater.* **247** 46–9

[20] Martin P, Ripert M, Carlot G, Parent P and Laffon C 2004 A study of molybdenum behaviour in UO_2 by x-ray absorption spectroscopy *J. Nucl. Mater.* **326** 132–43

[21] Kleykamp H, Paschoal J O, Pejsa R and Thummler F 1985 Composition and structure of fission product precipitates in irradiated oxide fuels: correlation with phase studies in the Mo–Ru–Rh–Pd and $BaO–UO_2–Zr_2–Mo_2$ systems *J. Nucl. Mater.* **130** 426–33

[22] Walker C T, Bagger C and Mogensen M 1996 Observations on the release of cesium from UO_2 fuel *J. Nucl. Mater.* **240** 32–42

[23] Lindemer T B and Besmann T M 1981 Thermodynamic review and calculations—alkali-metal oxide systems with nuclear fuels, fission products, and structural materials *J. Nucl. Mater.* **100** 178–226

[24] Cordfunke E H P and Konings R J M 1990 *Thermochemical Data for Reactor Materials and Fission Products* (Amsterdam: North-Holland)

[25] Huang J, Yamawaki M, Yamaguchi K, Ono F, Yasumoto M, Sakurai H and Sugimoto J 1999 Vaporisation properties of $Cs_2U_4O_{12}$ in LWR severe accident simulation conditions *J. Nucl. Mater.* **270** 259–64

[26] Maeda K, Tanaka K, Asaga T and Furuya A 2005 Distributions of volatile fission products in or near the fuel-cladding gap of the FBR MOX fuel pins irradiated to high burn-up *J. Nucl. Mater.* **344** 274–80

[27] Kresse G and Joubert D 1999 From ultrasoft pseudopotentials to the projector augmented-wave method *Phys. Rev.* B **59** 1758–75

[28] Kresse G and Furthmüller J 1996 Efficiency of *ab initio* total energy calculations for metals and semiconductors using a plane-wave basis set *Comput. Mater. Sci.* **6** 15–50

[29] Dudarev S L, Botton G A, Savrasov S Y, Humphreys C J and Sutton A P 1998 Electron energy loss spectra and the structural stability of nickel oxide: an LSDA + U study *Phys. Rev.* B **57** 1505

[30] Dudarev S L, Nguyen Manh D and Sutton A P 1997 Effect of Mott–Hubbard correlations on the electronic structure and structural stability of uranium dioxide *Phil. Mag.* B **75** 613–28

[31] Laskowski R, Madsen G K H, Blaha P and Schwarz K 2004 Magnetic structure and electric-field gradients of uranium dioxide: an *ab initio* study *Phys. Rev.* B **69** 140408

[32] Schoenes J 1987 Recent spectroscopic studies of UO_2 *J. Chem. Soc. Faraday Trans.* II **83** 1205–13

[33] Kotani A 1992 Systematic analysis of core photoemission spectra for actinide di-oxides and rare-earth sesqui-oxides *Prog. Theor. Phys. Suppl.* **108** 117–31

[34] Spino J, Rest J, Goll W and Walker C T 2005 Matrix swelling rate and cavity volume balance of UO_2 fuels at high burn-up *J. Nucl. Mater.* **346** 131–44

[35] Iwasawa M, Chen Y, Kaneta Y, Ohnuma T, Geng H Y and Kinoshita M 2006 First-principles calculation of point defects in uranium dioxide *Mater. Trans.* **47** 2651–7

[36] Knudin K N, Scuseria G E and Martin R L 2002 Hybrid density-functional theory and the insulating gap of UO_2 *Phys. Rev. Lett.* **89** 266402

[37] Matzke Hj 1987 Atomic transport properties in UO_2 and mixed oxides (U, Pu)O_2 *J. Chem. Soc. Faraday Trans.* II **83** 1121–42

[38] Lidiard A B 1966 Self-diffusion of uranium in UO_2 *J. Nucl. Mater.* **19** 106–8

[39] Geng H Y, Chen Y, Kaneta Y, Iwasawa M, Ohnuma T and Kinoshita M 2008 Point defects and clustering in uranium dioxide by LSDA + U calculations *Phys. Rev.* B **77** 104120

[40] Busker G, Grimes R W and Bradford M R 2000 The diffusion of iodine and caesium in the $UO_{2\pm x}$ lattice *J. Nucl. Mater.* **279** 46–50

[41] Phillips J R, Waterbury G R and Vanderborgh N E 1974 Distribution of ^{134}Cs and ^{137}Cs in the axial UO_2 blankets of irradiated (U, Pu)O_2 fuel pins *J. Inorg. Nucl. Chem.* **36** 17–23

[42] Cheynet B, Chaud P and Fischer E 2004 Base de données thermodynamiques Cs–Mo–O–U *Technical Report 1* ©Thermodata 2003–2008—NUCLEA Database

[43] Kittel C 1996 *Introduction to Solid State Physics* 7th edn (New York: Wiley)

[44] Simmons G and Wang H 1971 *Single Crystal Elastic Constants and Calculated Aggregate Properties: a Handbook* 2nd edn (Cambridge, MA: MIT Press)

[45] Gschneider K A 1964 *Solid State Phys.* **16** 275–426

[46] Vannerberg N G 1962 *Progress in Inorganic Chemistry* vol 4, ed F A Cotton (New York: Wiley-Interscience) chapter (Peroxides Superoxides and Ozonides of the Metals of Groups Ia, IIa, and IIb) pp 125–97

[47] Fee D C and Johnson C E 1981 Cesium thermomigration and reaction in nuclear fuels *J. Nucl. Mater.* **96** 71–9

[48] Furuya H, Ukai S, Shikakura S, Tsuchiuchi Y and Idemitsu K 1993 Axial distribution of cesium in heterogeneous FBR fuel pins *J. Nucl. Mater.* **201** 46–53

[49] Yagnik S K, Machiels A J and Yang R L 1999 Characterisation of UO_2 irradiated in the BR-3 reactor *J. Nucl. Mater.* **270** 65–73

[50] Matzke Hj 1994 Oxygen potential in the rim region of high burn-up UO_2 fuel *J. Nucl. Mater.* **208** 18–26

[51] Ugajin M, Nagasaki T and Itoh A 1996 Contribution to the study of the Cs–U–Mo–I–O system *J. Nucl. Mater.* **230** 195–207